JOURNAL OF GEOPHYSICAL RESEARCH, VOL. 99, NO. D8, PAGES 16,633–16,642, AUGUST 20, 1994

Comparison of measured OH concentrations with model calculations

D. Poppe, J. Zimmermann, R. Bauer, T. Brauers, D. Brüning, J. Callies, H.-P. Dorn, A. Hofzumahaus, F.-J. Johnen, A. Khedim, H. Koch, R. Koppmann, H. London, K.-P. Müller, R. Neuroth, C. Plass-Dülmer, U. Platt, F. Rohrer, E.-P. Röth, J. Rudolph, U. Schmidt, M. Wallasch, and D. H. Ehhalt

Institute for Atmospheric Chemistry, Forschungszentrum Jülich, Jülich, Germany

Abstract. The influence of chemical precursors and sunlight on the atmospheric OH abundance is investigated by a comparison of locally measured tropospheric OH with model calculations. The latter are based on the gas phase reaction mechanism of the regional acid deposition model (RADM2) which incorporates an explicit inorganic and a comprehensive organic chemistry. The experimental data were obtained in the planetary boundary layer during two sets of campaigns. In Deuselbach (1983) and Schauinsland (1984), rural conditions were encountered with NO_x concentrations on the average of 2.2 and 0.9 ppb, respectively. This data set was already compared with model calculations based upon an older and less detailed chemical reaction scheme (Perner et al., 1987). Since then the experimental data were reanalyzed leading to modified measured OH concentrations and also to modified precursor concentrations. For a consistent comparison with the more recent campaigns in Jülich (1987 and 1988) we have redone the calculations. The modeled and measured OH concentrations of the campaigns in 1983 and 1984 correlate well with a coefficient of correlation of $r = 0.73$. The model overpredicts OH by about 20%. Under more polluted conditions in Jülich with average NO_x concentrations of 4 ppb the correlation coefficient between experimental and modeled data are significantly smaller ($r = 0.61$). Possible reasons are the influence of not measured precursors, for example isoprene, and the inapplicability of a quasi-steady state model under the spatially inhomogeneous conditions in Jülich. Again the model overpredicts the OH concentration by about 15%, which is somewhat smaller than for the rural case. The precision of the comparison is limited by the uncertainties of the chemical reaction rate constants.

1. Introduction

Experimental and model work has provided increasing evidence that the hydroxyl radical OH is the most important oxidizing reagent in the lower atmosphere during daytime [*Levy*, 1971, 1972; *Ehhalt et al.*, 1991]. It is produced by the photolysis of ozone at wavelengths below 320 nm

(R1) $$O_3 + h\nu \rightarrow O(^1D) + O_2$$

generating electronically excited oxygen atoms, $O(^1D)$. Their excitation energy (~2 eV) opens a reaction channel with water vapor molecules to form OH radicals

(R2) $$O(^1D) + H_2O \rightarrow 2\ OH$$

The hydroxyl radical reacts with most atmospheric trace gases initiating their oxidation and eventual removal from the troposphere through subsequent chemical processes. For many compounds the rate-determining step of this degradation is the reaction with OH so that their tropospheric lifetime is determined by the OH concentration. As a consequence, changes of the OH concentration would result in corresponding changes of the atmospheric trace gas concentration. In addition, the net chemical production of ozone in the troposphere depends nearly linearly on the destruction rate of CO, CH_4, and other nonmethane hydrocarbons (NMHC) by OH given sufficient NO_x, which underlines again the importance of OH. In fact, any change of the tropospheric OH concentration has its impact on many aspects of atmospheric chemistry. Chemical models based on laboratory kinetic studies and atmospheric observations have provided insight into the couplings of the chemical system in the atmosphere [*Logan et al.*, 1981; *Weinstock et al.*, 1980; *Ehhalt*, 1986, 1987; *Liu et al.*, 1987; *Stockwell et al.*, 1990; *Thompson et al.*, 1990; *Poppe et al.*, 1992, 1993a] and have identified the chemical processes and meteorological parameters which control the OH abundance. It could be shown that the chemistry of OH is to a varying degree coupled to all trace gases, in particular to the nitrogen oxides, ozone, and the hydrocarbons.

The ultimate test of the applicability of such models and their validity for the atmosphere is a comparison of model calculations with measured tropospheric OH concentrations. Here we will analyze local measurements of OH

Paper number 94JD00378.
0148-0227/94/94JD-00378$05.00

performed in near-surface air during summer periods in rural and moderately polluted environments in Germany.

Such a comparison is simplified by the fact that OH and the peroxy radicals have short lifetimes because of their high reactivity. Transport of short-lived compounds does not contribute significantly to their local concentration so that a zero-dimensional model with no spatial resolution suffices to describe the fast chemical processes. Quasi-steady state concentrations are attained within minutes and the OH concentration is solely determined by the concentrations of longer-lived reactands and meteorological parameters. These support data have to be measured simultaneously in order to make a comparison of experimental and model OH data meaningful. At this stage only those processes need to be addressed which dominantly influence the OH concentration.

2. Strategy of Measurement and Comparison

The chemistry of OH and the associated peroxy radicals dictate the strategy for a meaningful comparison of calculated and modeled OH concentrations. The kinetics of the radicals are strongly coupled and box model calculations show that the time T needed to reach stationarity for OH, the peroxy radicals, and photostationarity for NO and NO_2 is of the order of 1 minute. Since the integration time of the OH measurement was much larger than T and varied between 10 min and several hours, the experiments could not resolve transient effects in the local concentrations. Therefore stationarity of the radical concentrations is assumed for the comparison with the model. Consequently, the experimental site should display horizontal uniformity so that air parcels passing the site have experienced constant chemical and meteorological conditions for at least T to attain quasi-steady state concentrations. For example, with a wind speed of 5 m/s and T = 1 min this requirement implies horizontal homogeneity over at least 300 m. Vertical transport and dry deposition influence the local OH budget in two ways. Firstly, the highly reactive OH and peroxy radical are expected to be effectively deposited at the surface. Secondly, the gradients of the chemical precursors induce additional fluxes of OH. Thus the local chemical budget of OH a few meters aboveground can be considerably perturbed by transport. Because of the high variability of these fluxes it is very difficult to model quantitatively the influence on OH. Therefore measurements should also take place well off the ground. The experimental data of OH must be accompanied by measurements of the longer-lived precursors and meteorological parameters in the same mass of air. Then a zero-dimensional transport independent model is adequate for the comparison.

3. Field Data

There are only very few data sets available for an intercomparison of modeled and calculated OH concentrations since the direct detection of atmospheric OH is very difficult. Overviews of the experimental techniques and the existing data of measured atmospheric OH concentrations are given by *Altshuller* [1989] and *Hewitt and Harrison* [1985]. The Institute of Atmospheric Chemistry in Jülich is one of the groups that have performed simultaneous measurements of OH and the necessary support data to characterize the air mass containing OH. With respect to the applied measurement techniques for OH and other trace gases the reader is referred to *Perner et al.* [1987], *Platt et al.* [1987, 1988], *Dorn et al.* [1988], *Callies* [1988], *Junkermann et al.* [1989], and *Hofzumahaus et al.* [1991]. Recently, *Mount* [1992] and *Comes* [1992] performed OH measurements in rural air utilizing similar techniques. *Felton* [1988] and *Felton et al.* [1988, 1990] conducted campaigns utilizing the in situ ^{14}C method for OH. They measured only a small set of support data which makes the comparison with model calculations rather uncertain. *Eisele and Tanner* [1991] determined [OH] by mass spectrometry, however, no support data were reported.

Our field data were obtained at three different locations in Germany. All campaigns were conducted during summertime in meteorologically steady conditions with bright sunshine. Moreover, the visibility was always good as it is required by the applied long-path absorption technique for OH.

The 1983 campaign took place in Deuselbach at a rural station at 480 m in altitude [*Perner et al.*, 1987] with negligible pollutant sources nearby. The long-path absorption technique probed air in 55 m aboveground on the average.

The field experiment in 1984 was conducted at Schauinsland, a mountain station about 1300 m above sea level in the Black Forest. Because of its altitude the station experiences very different air masses during the day since the site is above the planetary boundary layer (PBL) in the morning hours, while in the early afternoon it is within the PBL because of the increased height of the mixing layer. The OH data were taken in 200 m height above ground on the average. Both stations exhibited relatively low nitrogen oxides and NMHC concentrations during the campaigns. For example, $[NO_2]$ varies between 0.4 ppb and 2 ppb, while ethene abundances were between 0.3 ppb and 1 ppb.

The campaigns in 1987 and 1988 were located in Jülich at 100 m altitude. Jülich is a rural site with some small paper mills and chemical factories. It is surrounded by nearby sources of trace gases from automobile exhaust and small chemical research facilities. The area exhibits rather high NMHC and NO_2 concentrations, the latter varying between 2 ppb and more than 10 ppb during both field experiments. OH was probed in 60 m height above the surface.

During both types of campaigns, most of the important inorganic precursors of OH like NO_2, O_3, H_2O, and the photolysis frequencies of O_3 and NO_2 were monitored continuously. The measured set of organic compounds and the measurement frequencies, however, were very different for the campaigns. For example, in 1983 and 1984 many NMHCs, even the reactive species, were measured only once or twice per day and PAN measurements were not done at all. Also, often the data do not refer to the same time with the same interval of integration. Sometimes the time elapsed between the OH and the precursor measurements exceeds several hours. Then the data were completed, in particular, for acetaldehyde, propane, and CO during the early campaigns in 1983/1984 and also for the Jülich data of 1987. The completion was based on the experimental data of the 1988 campaign [*Poppe et al.*, 1993b] when the hydrocarbons and all other parameters were measured on a regular basis several times per day. The anthropogenic hydrocarbons, CO, and NO_x are positively correlated with correla-

tion coefficients, r, larger than 0.7 with typical values of 0.8. A linear regression analysis [*Wallasch et al.*, 1993] allows to estimate missing precursor concentrations. Even after completion the data sets are inhomogeneous with respect to the set of measured organic compounds. A possible influence of this inhomogeneity on the calculated OH concentrations should be excluded in order to make the campaigns intercomparable. Therefore only a common subset of precursors were selected for the desired comparison which were measured during all campaigns. These experimental data were compiled in Table 1 (see also *Poppe et al.* [1994]).

4. Chemical Reaction Scheme

The gas phase chemistry of the regional acid deposition model (RADM2) was chosen to model the OH concentration. The chemical scheme contains an explicit organic chemistry for hydrocarbons up to C_2 and treats all higher NMHC in a lumped fashion [*Stockwell et al.*, 1990; *Middleton et al.*, 1990]. It was designed primarily for rural but also polluted environments and is therefore applicable to all campaigns. The comparison of the RADM2 with several other recent reaction schemes by *Hough* [1988] and *Dodge* [1989] showed quantitative agreement for OH and various other short-lived compounds among the different formulations of the chemistry despite the considerable differences in the implementations of the organic reactions.

Input for the model are the experimental data for the long-lived precursors and the photolysis frequencies. Obviously, the model requires more parameters to be specified than are available from the measurements.

The missing data fall into three categories. Firstly, those that are known from model calculations to be of little influence on OH, so that their actual values are not crucial. The photolysis of organic peroxides and H_2O_2 produces OH and peroxy radicals. However, their mixing ratios are not likely to exceed several ppb so that their contribution is still small compared to the production from (R1) and (R2). Degradation products of the hydrocarbons for example, which react very slowly or not at all with either OH or the peroxy radicals, belong also to this category.

Secondly, glyoxal, methylglyoxal, dicarbonyls, and ketones, which are produced during the oxidation of several higher NMHCs, react quickly with OH and are therefore potentially important. Higher NMHCs belong to this group, too. For the comparison presented here the influence of these compounds was neglected by assigning vanishing concentrations (see section 5.2). Thirdly, they are known to be important for OH. The photolysis frequencies of formaldehyde and acetaldehyde fall into this group. Their J values are calculated from the experimental ozone photolysis frequency by scaling with the calculated photolysis data from a photon flux model [*Röth*, 1994].

As already mentioned in section 3, only a subset of NMHC was taken as measured to treat all campaigns on the same basis. All others were included by relating their mixing ratios to those of propane, ozone, and NO_2 used as leading factors. The equations are entered into Table 2. They were taken from an analysis of the corresponding correlations deduced from the comprehensive hydrocarbon database of the Jülich campaign in 1988 [*Wallasch et al.*, 1994]. The diurnal cycles of several hydrocarbons (methane, ethane, propane, *n*-butane, *i*-butane, *n*-pentane, *i*-pentane, ethene, propene, 1-butene, ethine, benzine, toluene, *o*-xylene, *p*/*m*-xylene) were measured. The relations were slightly modified for the Deuselbach campaign (1983) to meet the observation of relatively high alkene mixing ratios during that period. For PAN the correlation was taken with the exception of 1988, when measured PAN concentration were available. The relations are entered into Table 2 together with estimated errors. *Poppe et al.* [1994] have shown that this approximate treatment of precursors do not lead to substantial differences in the modeled OH concentrations by comparing calculations adopting the relations of Table 2 and using the full measured hydrocarbon data set.

The concentrations of the short-lived compounds are calculated in the steady state approximation using these data as input. Short-lived species are oxygen atoms, OH, HO_2, and all peroxy radicals associated with the oxidation of hydrocarbons. The nitrogen compounds HONO, NO_3, N_2O_5, HNO_4, and also NO are treated as steady state species using the full chemical scheme of RADM2, that includes, in particular, the NO losses due to reactions with the peroxy radicals. All other species included into the scheme are fixed parameters, as specified from the experiments.

5. Comparison of Measurements With Calculated OH Concentrations

5.1. Campaigns in Rural Environments

The earlier campaigns of Deuselbach (1983) and Schauinsland (1984) are the simpler case. From (R1) and (R2) one would predict a dependence of [OH] on the photolysis of ozone. Indeed, the diurnal cycle of the measured OH concentration and the photolysis rate (Figure 1) vary in parallel. This relation is shown more clearly and quantitatively in Figure 2, where the measured OH data at Deuselbach and Schauinsland are plotted against the photolysis rate of (R1) denoted by J_1. The correlation coefficient, $r(\mathrm{OH}, J_1)$, is 0.76 with a 95% confidence interval of 0.43, . . . , 0.91; r^2 $(\mathrm{OH}, J_1) = 0.58$ is the fraction of the total variance of [OH] that can be explained by a linear dependence on J_1. The remaining variance stems from the experimental uncertainty of OH and J_1 and from the influence of other precursors and parameters on which the OH concentration depends. In-

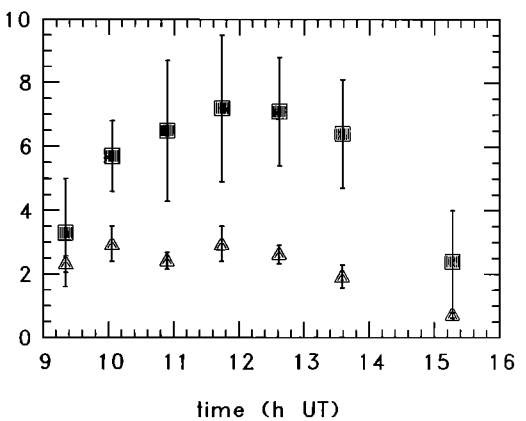

Figure 1. Diurnal variation of the measured OH concentration (squares) in units of 10^6 cm^{-3} and the photolysis frequency of ozone (triangles) in units of 10^{-5} s^{-1} at Schauinsland, June 25, 1984.

Table 1. Experimental Data of the Campaigns in Deuselbach (1983), Schauinsland (1984), and Jülich (1987/1988)

No.	Date	UT	H_2O[a]	JO_3[b]	JNO_2[c]	T/C	O_3[d]	NO_2[d]	HCHO[d]	CH3CHO[d]	C_3H_8[d]	CO[d]	PAN[d]
						1983 Deuselbach							
1	May 17	0938	2.74	0.78	3.60	14.5	41	2.20	0.90	0.60[e]	0.70[e]	270	···
2	May 18	1132	2.11	1.64	7.60	17.2	40	7.80	0.70[e]	0.60[e]	1.00[e]	360	···
3	May 18	1304	2.08	1.08	5.70	17.0	42	3.60	0.70[e]	0.50[e]	0.70[e]	280	···
4	May 18	1458	1.96	0.55	5.00	17.2	46	1.30	0.70	0.50[e]	0.50	240	···
5	May 19	1212	2.10	1.26	6.20	15.0	48	1.00	0.30	0.20[e]	0.50	260	···
6	May 19	1352	2.03	0.97	6.10	16.2	50	0.60	0.30	0.20[e]	0.40	230	···
7	May 19	1457	1.96	0.67	5.90	16.4	52	0.60	0.30	0.20[e]	0.40	220	···
8	May 20	0918	2.27	1.14	6.50	18.5	53	1.60	0.50	0.40[e]	0.60[e]	290	···
9	May 20	1117	2.13	1.86	8.00	21.9	57	1.50	0.60	0.50[e]	0.54	250	···
Mean			2.15	1.11	6.07	17.1	47	2.24	0.56	0.41	0.59	267	
						1984 Schauinsland							
10	June 25	0920	1.65	2.30	8.20	10.5	50	0.40	0.60	0.08	0.39	230[e]	···
11	June 25	1003	1.62	2.90	8.80	10.5	49	0.63	0.63	0.10[e]	0.50[e]	230[e]	···
12	June 25	1053	1.56	2.40	6.70	10.2	49	1.00	0.33	0.13[e]	0.52	230[e]	···
13	June 25	1144	1.66	2.90	7.80	11.6	47	0.81	0.42	0.16[e]	0.52	230[e]	···
14	June 25	1236	1.67	2.60	7.30	11.0	50	0.59	0.59	0.18	0.50[e]	230[e]	···
15	June 25	1335	1.75	1.90	6.60	10.5	49	0.54	0.68	0.19[e]	0.50[e]	230[e]	···
16	June 25	1516	1.93	0.70	3.50	11.2	48	0.75	0.73	0.20[e]	0.50[e]	230[e]	···
17	June 26	1151	2.42	2.00	5.80	14.7	47	2.20	1.20	0.29	0.63	350[e]	···
Mean			1.80	2.21	6.84	11.3	49	0.92	0.65	0.17	0.51	245	
						1987 Jülich							
18	July 5	1058	3.20	2.30	7.80	23.1	48	4.40	0.80	0.80[e]	1.53	309	···
19	July 5	1254	3.20	2.09	7.30	24.1	54	4.00	0.80	0.80[e]	1.50[e]	300[e]	···
20	July 5	1354	3.10	1.74	6.80	24.6	62	4.50	1.20	1.00[e]	1.50[e]	300[e]	···
21	July 5	1427	3.00	1.43	6.30	24.8	60	4.30	1.40	1.00[e]	1.50[e]	300[e]	···
22	July 5	1510	2.90	1.05	5.80	24.9	59	3.70	1.40	1.00[e]	1.50[e]	250[e]	···
23	July 11	0915	3.30	1.46	5.80	23.1	56	5.70	1.00	1.00[e]	1.80[e]	300[e]	···
24	July 11	1032	3.10	2.05	6.80	24.0	53	5.00	1.20	1.00[e]	1.80[e]	300[e]	···
25	July 11	1131	3.01	2.19	7.00	24.7	29	2.10	0.75	0.70[e]	1.00[e]	189	···
26	July 11	1231	3.50	1.84	6.40	25.0	33	2.20	0.70	0.70[e]	1.00[e]	200[e]	···
27	July 11	1436	3.90	1.21	5.60	25.7	54	3.80	1.25	0.70[e]	1.00[e]	200[e]	···
28	July 14	1117	3.50	2.19	6.90	22.6	56	4.00	1.00	0.70[e]	1.10	189	···
29	July 14	1210	3.50	2.24	7.00	23.3	63	2.70	0.90	0.70[e]	1.10	189	···
30	July 14	1243	3.40	2.15	6.90	23.5	67	2.30	0.80	0.70[e]	1.10[e]	190[e]	···
31	July 14	1342	3.40	1.52	5.80	24.3	73	2.30	0.90	0.70[e]	1.10[e]	200[e]	···
32	July 14	1406	3.40	1.57	5.80	24.6	75	2.70	1.00	0.70[e]	1.10[e]	200[e]	···
33	July 14	1433	3.80	1.28	5.60	24.7	78	2.90	1.00	0.70[e]	1.10[e]	200[e]	···
34	July 14	1515	3.80	0.90	4.90	24.8	82	2.60	1.00	0.70[e]	1.10[e]	200[e]	···
Mean			3.35	1.72	6.38	24.2	59	3.48	1.01	0.80	1.28	236	
						1988 Jülich							
35	May 15	1304	2.70	1.18	4.47	25.1	73	2.44	2.03	0.29	1.08	243	1.25
36	May 15	1335	2.69	0.76	3.24	24.7	72	2.86	1.87	0.29	1.05	246	1.45
37	May 15	1412	2.74	0.57	2.74	24.7	71	2.30	1.71	0.29	1.02	258	1.54
38	May 15	1453	2.79	0.44	2.55	24.6	70	2.59	1.60	0.27	1.11	258	1.49
39	May 15	1615	2.76	0.15	1.42	24.0	73	2.91	1.57	0.24	1.26	265	1.60
40	May 31	1147	2.11	1.33	5.16	14.9	40	5.34	0.66	0.04	0.42	191	0.24
41	May 31	1203	2.01	1.48	6.06	15.1	39	5.35	0.65	0.04	0.41	197	0.24
42	May 31	1225	2.13	1.06	4.39	15.3	38	5.00	0.64	0.17	0.44	200	0.28
43	May 31	1447	2.19	0.76	4.95	15.4	39	3.81	0.56	0.50	0.63	233	0.46
44	May 31	1458	2.21	0.70	4.69	15.4	39	3.74	0.56	1.00	0.64	274	0.49
45	May 31	1519	2.16	0.60	4.44	15.9	39	3.66	0.56	0.50	0.64	229	0.49
46	May 31	1558	2.33	0.09	0.84	14.2	39	6.16	0.56	0.50	0.63	236	0.57
47	June 2	1340	3.42	0.59	2.07	15.3	21	9.64	0.73	0.08	0.61	217	0.37
48	June 2	1352	3.41	0.53	1.92	15.4	21	10.00	0.77	0.09	0.60	224	0.39
49	June 2	1406	3.38	0.32	1.22	15.1	20	10.48	0.81	0.09	0.60	227	0.42
50	June 4	0854	2.54	0.90	4.67	14.7	38	3.16	0.21	0.20	0.50	191	0.18
51	June 4	1015	2.48	1.34	5.69	15.4	41	3.01	0.44	0.20	0.50	191	0.25
52	June 4	1024	2.37	1.37	5.78	15.8	41	3.04	0.47	0.20	0.50	191	0.27
53	June 4	1034	2.33	1.57	6.44	16.0	41	3.07	0.50	0.20	0.50	191	0.28
54	June 4	1131	2.22	1.50	5.85	15.9	41	3.14	0.42	0.20	0.50	183	0.31
55	June 4	1150	2.31	0.97	3.77	15.6	41	3.10	0.35	0.20	0.50	189	0.30
56	June 4	1208	2.30	1.53	6.06	16.2	41	3.07	0.50	0.20	0.50	182	0.31
57	June 4	1216	2.30	1.55	6.17	16.5	41	3.22	0.57	0.20	0.50	184	0.32
58	June 4	1230	2.31	1.47	6.05	16.7	42	3.39	0.66	0.21	0.47	185	0.35
59	June 4	1241	2.30	1.62	6.75	17.0	41	3.54	0.75	0.20	0.47	185	0.35
60	June 4	1257	2.33	0.78	3.07	16.6	41	3.77	0.72	0.20	0.48	185	0.40
61	June 4	1305	2.64	0.97	4.21	14.6	41	3.67	0.70	0.19	0.48	191	0.39
62	June 4	1319	2.83	0.54	2.13	14.4	41	3.45	0.68	0.18	0.49	182	0.36
63	June 5	1154	2.17	1.14	4.77	14.9	41	3.05	0.40	0.09	1.23	170	0.50

Table 1. (continued)

No.	Date	UT	H_2O[a]	JO_3[b]	JNO_2[c]	T/C	O_3[d]	NO_2[d]	HCHO[d]	CH3CHO[d]	C_3H_8[d]	CO[d]	PAN[d]
64	June 5	1218	2.12	1.34	5.64	14.0	43	2.87	0.43	0.09	1.10	173	0.47
65	June 5	1240	2.04	1.38	5.94	15.0	45	2.70	0.46	0.09	1.07	167	0.54
66	June 5	1253	2.08	0.96	4.31	15.4	46	2.59	0.47	0.09	1.00	167	0.59
67	June 5	1304	2.17	0.45	2.11	14.4	46	2.59	0.48	0.09	0.99	173	0.61
68	June 5	1352	2.14	0.94	4.75	15.7	46	2.71	0.62	0.09	0.82	167	0.74
69	June 5	1403	2.11	1.10	6.14	15.9	45	2.73	0.70	0.09	0.78	168	0.70
Mean			2.43	0.97	4.30	16.7	45	3.96	0.73	0.22	0.70	204	0.57

All parameters were measured locally at one end of the absorption path of the OH measurement with the exception of O_3, NO_2, and HCHO, which were measured by differential optical absorption spectroscopy probing the same volume of air as the OH measurement. Time is given in UT.

[a]In units of 10^{17} cm^{-3}.
[b]In units of 10^{-5} s^{-1}.
[c]In units of 10^{-3} s^{-1}.
[d]In ppb.
[e]Marks estimates.

deed, the model predicts a much larger correlation between the calculated OH (denoted by subscript c) and the measured ozone photolysis frequency with $r(OH_c, J_1) = 0.90$. Measured and calculated OH concentrations are compared in Figure 3. The error bars of the experimental data display the 1-sigma error of an individual measurement. Systematic errors for example from the uncertainty of the OH absorption cross section are not taken into account. Each individual precursor has uncertainties from two sources. Firstly, there is the experimental uncertainty of the individual measurements. Secondly, there is an uncertainty due to the fact that measurements of OH and its precursors are not strictly simultaneous and not in the same mass of air. For example, OH is determined with the long-path absorption technique sampling a volume of several kilometers in length and a diameter of less than a meter. The appropriate photolysis frequency is then the temporal and spatial average in this volume during the integration time of the OH experiment. However, the measurement of J_1 took place at one end of the absorption path. As a measure of the statistical deviation between in situ and long-path result, we adopted the 10-min variance of the in situ J_1. Similar arguments hold for the other support data. Both types of errors were compiled by *Poppe et al.* [1994].

The errors of the modeled OH were calculated solely from the propagation of these uncertainties. They were sampled by a simple Monte Carlo technique. The error bars of the model are taken from the square root of the variance of the modeled OH_c. The dominating terms for the uncertainty of OH_c stem from the experimental errors of J_1, O_3, NO_2, HCHO, and CO. Systematic errors due to the uncertainties of the rate constants were not considered. The mean $\langle[OH_c]\rangle$ and median $[OH_c]_m$ were also calculated. A priori it is not clear whether $\langle[OH_c]\rangle$ or $[OH_c]_m$ give the more appropriate choice for the modeled hydroxyl concentration. For reasons of simplicity we rely on $[OH_c]$, which is always directly determined from experimental input. It should be noted that $[OH_c]_m$ reflects more realistically the influence of experimental uncertainties and the spatial distribution of the precursors along the light path. Worst case estimates of the influence of a spatially inhomogeneous NO_x concentrations were already discussed by *Platt et al.* [1988]. The nonlinear dependencies of the OH concentration in particular on $[NO_x]$ induce a systematic deviation of $\langle[OH_c]\rangle$ and $[OH_c]_m$

Table 2. Relations Used to Calculate the Model Input Data for the Hydrocarbons

Species[a]	Relation	Error	r
ETH(C_2H_6)	$2 + 0.3*C_3H_8$	1.5	0.86
HC3[b]	$3.0*C_3H_8$	1.5	0.84
HC5[c]	$1.5*C_3H_8$	1.5	0.33
OL2(C_2H_4)[g]	$a*C_3H_8$	2.0	0.20
OLT[d]	$0.3*C_2H_4$	2.0	−0.07
TOL[e]	$0.3*C_2H_4$	2.0	−0.3
XYL[f]	0.1*TOL	2.0	−0.53
PAN	$0.003*NO_2*O_3$/ppb	2.0	0.29

Units of ppb are used.
[a]Regional acid deposition model (RADM2) species. Chemical notation in parentheses.
[b]Alkanes with OH rate constant (298,1 atm) between 2.7×10^{-13} and 3.4×10^{-12} cm^3 s^{-1}.
[c]Alkanes with OH rate constant (298,1 atm) between 3.4×10^{-12} and 6.8×10^{-12} cm^3 s^{-1}.
[d]Terminal alkenes.
[e]Toluene and less reactive aromatics.
[f]Xylene and more reactive aromatics.
[g]1984, $a = 2$; 1983, 1987, 1988, $a = 1$.

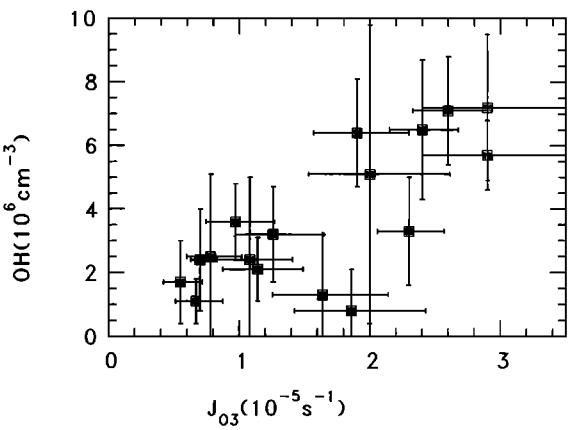

Figure 2. Correlation of measured OH concentrations with simultaneously observed frequencies of the photolysis of ozone from the Deuselbach (1983) and Schauinsland (1984) campaigns. Error bars indicate the mean standard deviation. (Correlation coefficient is 0.76.)

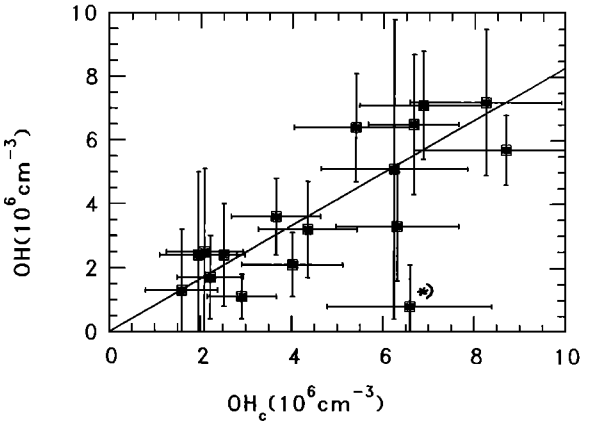

Figure 3. Correlation of measured and calculated OH concentrations at Schauinsland and Deuselbach. The error bars represent the mean standard deviations. The straight line is calculated from a least squares fit through the data and the origin disregarding the marked outlier. (Correlation coefficient is 0.73.)

from directly determined $[OH_c]$. For example, $[OH_c]_m$ is smaller than $[OH_c]$ by about 8% for the Deuselbach/Schauinsland data. The mean $\langle[OH_c]\rangle$ and median $[OH]_m$ practically coincide (the mean is 2% larger than the median for all campaigns). Since all three quantities are highly correlated ($r > 0.99$), a particular choice does not affect the correlation with the measured [OH]. Though Figure 3 shows positive correlation between [OH] and $[OH_c]$, the coefficient $r(OH, OH_c)$ is only 0.73 with a 95% confidence interval of 0.38, . . . , 0.89, i.e., not better than the one for the correlation between measured OH and J_1.

This is not surprising since the experimental uncertainty of the OH measurement already limits the degree of correlation that could be achieved (see appendix). Applying (A1) to [OH](=x), $[OH_c]$, (=y), and J_1 (=y) with $s_f = 2.0 \times 10^6$ cm^{-3} (accounting only for the experimental uncertainty of [OH] and neglecting the smaller errors of $[OH_c]$ and J_1, respectively) and $s_{OH} = 2.1 \times 10^6$ cm^{-3} leads to a mean upper bound of $r = 0.72$ in both cases. The comparison in Figure 3 validates the model in the sense that the calculated and measured OH concentrations agree in magnitude. There is, however, the tendency for the model to slightly overestimate the OH concentration. To quantify the overprediction we use a least squares fit

$$[OH] = a\,[OH_c] + b \qquad (1)$$

for a and b. Disregarding the outlier marked by an asterisk in Figure 3, we obtain $a = 0.83$ (± 0.05) if the offset b is suppressed and $a = 0.79$ (± 0.12), $b = 0.21$ (± 0.64) $\times 10^6$ cm^{-3} otherwise. The least squares minimization is not a statistically consistent estimator for the slope (see, for example, *Schneeweiß et al.* [1986]) since it underestimates the true a in the present case, where the independent variable, $[OH_c]$, has a finite error. In fact, [OH] and $[OH_c]$ have uncertainties of similar magnitude and cause. In such a case the change of [OH] to the independent variable gives another check of the slope

$$[OH_c] = a_c\,[OH] + b_c \qquad (2)$$

and provides a second value for $a = a_c^{-1} = 0.88$ (± 0.08) for $b = 0$ and $a = 1.06$ (± 0.2), $b = -1.0$ (± 0.65) $\times 10^6$ cm^{-3}. As discussed, the least squares fit underestimates a_c and therefore $a = a_c^{-1}$ overestimates the true a. Both estimates for b indicate that $b = 0$ is likely to be a good choice. Then the inverse fit of the slope in (2) nicely confirms the first estimate. On average the model overpredicts OH by 20%.

Note that the overprediction depends on the definition of $[OH_c]$. As already mentioned, the median of the OH_c distribution is smaller and would reduce the overprediction to 10%. In any case this difference is surprisingly small in view of the many experimental and statistical uncertainties.

Model calculations (see, for example, *Poppe et al.* [1993a]) predict a marked dependence of the OH concentration on the photolysis frequency of O_3 and the concentrations of ozone and water vapor because of the main production of OH from that photolysis followed by reaction of the emerging O^1D with water. Smaller production of radicals is provided by the photolysis of HCHO. Simultaneously, CO and HCHO destroy OH, the net effect on OH is reduced due to the back reaction of the produced HO_2 with NO. Its abundance under photostationarity depends on the NO_2 photolysis frequency. The correlations of these important precursors with the measured and modeled hydroxyl concentrations provide a further important test for the validity of the radical chemistry in the model (Figure 4). The actual values of the correlation coefficient depend very much on the campaign and sometimes seem to contradict chemical intuition. Strong correlations between the concentrations of the precursors of OH can overcompensate a dependence as it is inferred from sensitivity considerations. With exception of the temperature the absolute values of r for [OH] are smaller than for $[OH_c]$, which is to be expected, since experimental errors reduce the observed correlation. There is by and large good coincidence between both correlation coefficients which is further evidence for the validity of the chemical model. Only the correlations for ozone show a considerable difference, pointing possibly to yet unknown inaccuracies or incompleteness of the chemical scheme.

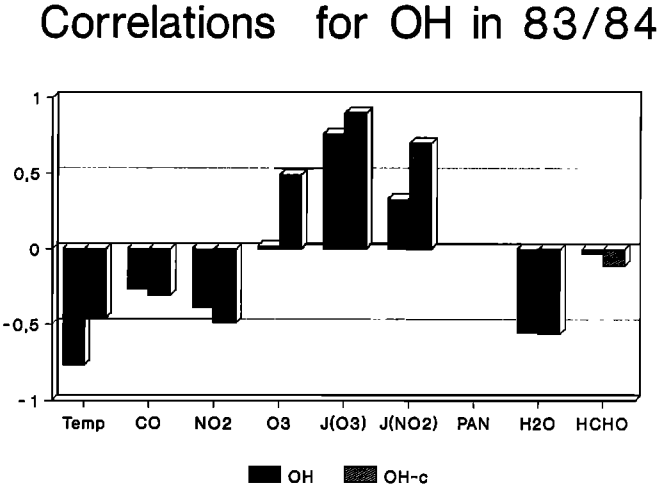

Figure 4. Correlations of several precursors with the calculated and the measured OH concentration.

5.2. Campaigns Under Moderately Polluted Conditions

Preliminary data of the campaigns in Jülich have already been discussed elsewhere [*Ehhalt et al.*, 1991]. Since then the calibration of the detector for the ozone photolysis has been improved, resulting in a small correction of the photolysis frequency, which has now an estimated total uncertainty of 26%. The dependence of the measured OH concentration on the measured ozone photolysis frequency is displayed in Figure 5. Since the OH concentrations are determined by a difference method, negative values may occur when the measured concentration approaches the 1-sigma uncertainty, which is indicated by the error bar. Despite instrumental improvements the OH measurements made in Jülich in 1987 and 1988 still show error bars as large as the earlier measurements. This is partly due to a shorter light path of only 6 km, while in 1983 and 1984 the pathlengths were 9.6 and 8.6 km, respectively. Moreover, the integration time for the OH measurement was reduced to improve the temporal resolution. Another reason is the presence of gases like SO_2 and HCHO which are known to have absorption features near the OH absorption lines. In addition, there are yet unidentified features within the spectral range of the OH lines which add to the current overall uncertainty. Identification and characterization of the unknown features will lead to smaller errors, possibly also to small changes in the measured OH concentrations. These changes, however, should well remain within the current error bars.

In contrast to the campaigns with a low burden of pollutants, we now observe a weaker correlation between measured OH and J_1 with $r(\mathrm{OH}, J_1) = 0.58$ and a 95% confidence interval of 0.36, . . . , 0.74, while the model gives $r(\mathrm{OH}_c, J_1) = 0.75$. Both correlations are smaller than for the low-pollution case (see section 5.1). This finding would be partly due to the lower average ozone photolysis frequency of $\langle J_1 \rangle = 1.2 \times 10^{-5}\ \mathrm{s}^{-1}$, whereas Deuselbach/Schauinsland had $\langle J_1 \rangle = 1.6 \times 10^{-5}\ \mathrm{s}^{-1}$), which tends to increase the relative importance of other OH radical sources. Assuming a linear relation according to (A1) with $s_{\mathrm{OH}} = 2.4 \times 10^6\ \mathrm{cm}^{-3}$ and $s_f = 2.0 \times 10^6\ \mathrm{cm}^{-3}$, we would obtain $r = 0.77$, which is larger than the experimental

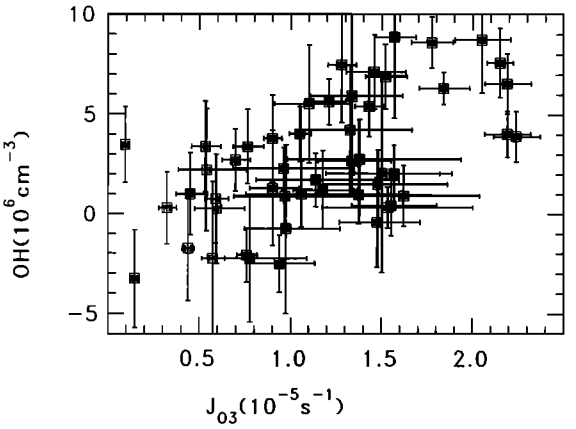

Figure 5. Correlation of measured OH concentrations with simultaneously observed frequencies of the photolysis of ozone from the Jülich (1987 and 1988) campaigns. Error bars indicate the mean standard deviation. (Correlation coefficient is 0.58.)

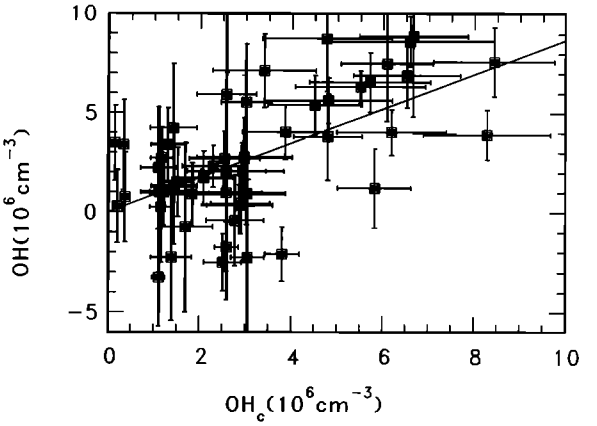

Figure 6. Correlation of measured and calculated OH concentrations at Jülich (1987 and 1988). The error bars represent the mean standard deviations. (Correlation coefficient is 0.61.)

correlation coefficient. Consequently, in addition to the known experimental uncertainties there must be other causes for the variance of the measured [OH]. The correlation diagram for measured and modeled OH (Figure 6) shows also a weak correlation with $r(\mathrm{OH}, \mathrm{OH}_c) = 0.61$ with a 95% confidence interval of 0.39, . . . , 0.76. Thus the chemistry as implemented in RADM2 and as initialized by the measured data does not help to explain the remaining variance of [OH].

The statistical model (1) adopting $b = 0$ is used to compare measured and modeled OH. The slope is $a = 0.87$, implying 15% overprediction by the model. This result is supported by comparing the mean values. The measured OH concentration is $2.7 \times 10^6\ \mathrm{cm}^{-3}$, while the mean calculated $[\mathrm{OH}_c]$ is given by $3.1 \times 10^6\ \mathrm{cm}^{-3}$, so that the model overpredicts OH concentrations by 15%. Previous comparisons by *Ehhalt et al.* [1991] and *Poppe et al.* [1992] have shown larger overpredictions. Since then, many of the OH absorption spectra were reanalyzed, which yields an average increase of the measured OH concentrations [*Poppe et al.*, 1993b].

The model overpredicts OH by the same amount for both types of campaigns. As stated already for the rural campaigns this discrepancy is surprisingly small in view of systematic uncertainties of the experiments and of the model due to the uncertainties of the rate constants.

We also investigated the correlations of precursors with the measured and modeled hydroxyl concentrations (Figure 7). Agreement between model and experiment implies agreement between corresponding correlation coefficients r. Similar to the rural campaigns the correlations for O_3 are different for experiment and model. In contrast to the rural campaigns there are additional discrepancies for NO_2, PAN, and HCHO pointing possibly to yet unknown inaccuracies or incompleteness of the chemical scheme which become effective under more polluted conditions. More specific conclusions can only be drawn from a larger data set. In the following we discuss possible causes for the small correlation between calculated and modeled OH for the Jülich data. One possible reason could be the simplified treatment of the NMHC discussed in section 4 and summarized in Table 2. This can be checked for the data form Jülich 1988. Calculations of $[\mathrm{OH}_c]$ using the correlations and using the full set of

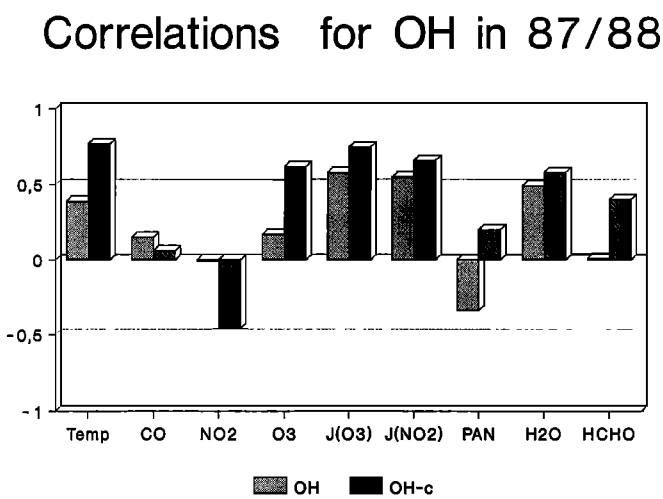

Figure 7. Correlations of several precursors with the calculated and the measured OH concentration.

measured hydrocarbons are compared. Excellent agreement with individual differences of the different OH_c not larger than 6% indicates that the approximate treatment of the measured hydrocarbons is not responsible for the remaining variance. Since some individual NMHC measurements deviate substantially from the approximate relations of Table 2, this result reflects the relatively small impact of the measured NMHC on the OH concentration.

Another possible reason is the neglect of the carbonyls, methylglyoxal, glyoxal, and the ketones, which are degradation products of the measured higher hydrocarbons. Their influence can be examined by introducing plausible values for their concentrations. Most likely, upper bounds are provided by their calculated steady state abundances for gas phase chemistry. Thus modeled OH concentrations correlate well ($r = 0.99$) with the previous calculations neglecting these compounds. The difference of 20% in the worst case is still small. Thus these compounds are not responsible for the extra variance.

Heterogeneous processes affecting the radical budget could be another cause for the unexplained variance. As an example, we discuss the loss of HO_2 radicals on aerosol surfaces. Adopting an aerosol surface density $F < 10^{-3}$ m^{-1} which is representative for continental clean air [*Withby*, 1978; *Logan et al.*, 1981], a thermal velocity of HO_2 of 110 m/s^{-1} and a sticking coefficient of unity, we obtain a decay rate $k < 0.11$ s^{-1} for the HO_2. This is an upper bound which is consistent with the lower bound of the sticking coefficient of 0.2 reported by *Mozurkewich et al.* [1987]. The correlation between [OH] and [OH_c] has been calculated as function of k. It is nearly independent of k, so that constant loss on aerosol offers no explanation for the extra variance. However, the slope a (according to (1) with $b = 0$) varies by a factor of 2 for $0.01\ s^{-1} < k < 0.1\ s^{-1}$, indicating that such a loss can generate variance provided the loss rate k is highly variable [*Poppe et al.*, 1994].

An additional possible cause for the discrepancy is the presence of emitted gases not measured and therefore not included into the model calculations. Measurements in rural and urban environments of the eastern United States, for example, have shown high concentrations of natural hydrocarbons, e.g., isoprene [*Martin et al.*, 1991]. The unaccounted influence of isoprene in concentrations observed there could be responsible for the present deviations between [OH] and [OH_c]. Figure 8 gives an estimate of the impact of isoprene by comparing [OH_c] calculated without isoprene and [OH_c] calculated with an isoprene mixing ratio of 4 ppb. Since the most important controlling parameter for isoprene emission, the temperature, was always below 26°C with an average of 19°C, this mixing ratio is likely to be too large and therefore the calculation gives an upper bound for this influence. Even a fixed isoprene concentration is capable of generating considerable variance with respect to the calculations without isoprene. The reason is that isoprene when present in the ppb range has such a severe impact on the partitioning of radicals between OH and HO_2 such that it can alter the relative importance of the radical loss by formation of HNO_3

$$\text{(R3)} \qquad OH + NO_2 + \text{air} \rightarrow HNO_3 + \text{air}$$

and the losses through reactions of HO_2 with HO_2 and RO_2

$$\text{(R4)} \qquad HO_2 + RO_2 \rightarrow \text{peroxides}.$$

Since the isoprene concentration, though likely to be much smaller than 4 ppb, was not measured, we cannot exclude isoprene as a contributor to the variance of [OH].

Finally, a source of variance is the possible inapplicability of a zero-dimensional model under the environmental conditions in Jülich. In contrast to the fairly homogeneous environment of the rural campaigns in Deuselbach and Schauinsland, the site in Jülich is rather structured with respect to pollutant sources. Spatial homogeneity is not always experienced by the air parcels passing the experimental site. In this case, the steady state assumption, which requires constant precursor concentrations and meteorological conditions within the parcel over several chemical relaxation times, is no longer valid. A study of the implications of nonstationarity on [OH] is in progress.

6. Summary

Measurements of the hydroxyl concentrations in chemically well characterized air masses have been compared with model calculations using a comprehensive reaction mecha-

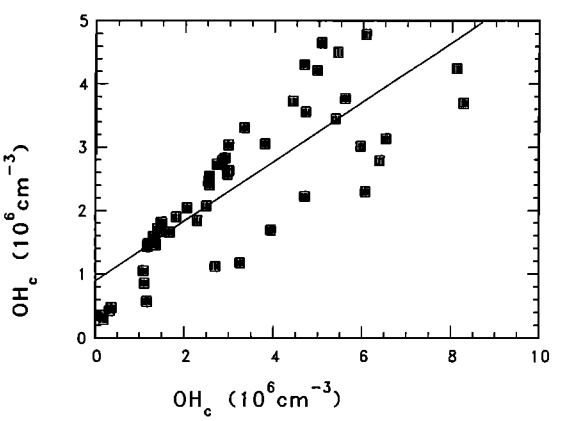

Figure 8. Influence of isoprene on the calculated OH concentration for the Jülich campaigns. [OH_c] for an isoprene mixing ratio of 4 ppb (ordinate) and [OH_c] for vanishing isoprene (abscissa).

nism for the gas phase chemistry of the troposphere. The comparison reveals agreement on the average for the field data from the campaigns under rural and moderately polluted conditions. The model slightly overpredicts OH by about 20%, which is well within the systematic uncertainties of the measured OH and calculated OH due to uncertain rate constants. Correlations of OH and OH_c with meteorological parameters, photolysis frequencies, and chemical precursors coincide so that the calculations also model these dependencies basically correct. Discrepancies in particular for O_3 indicate possible inadequacies of the model. However, since all these results are based on a statistical analysis of a relatively small number of data points, more data are needed before one could draw more firm and specific conclusions.

It should be pointed out that the study and its results are limited to near-surface air with weak and moderate pollutions. It should be complemented by investigations in different environments, for example the free troposphere and the marine boundary layer, to explore the OH chemistry for a wider range of chemical conditions.

Appendix

Consider a linear model in the statistical sense for the variables x and y

$$y = a(x + f) \tag{A1}$$

where f denotes the experimental errors of x and y. Neglecting f, the correlation coefficient, r, of x and y is unity. Including f yields a smaller r

$$r = 1/(1 + (s_f/s_x)^2)^{1/2} \tag{A2}$$

Here s_x^2 and s_f^2 are the true variances of x and f. Clearly, r in (A2) can be considered as an estimate for the true r if both variances are replaced by their corresponding estimates from a finite sample. Moreover, if not all experimental errors are included in f, r gives an estimate of a mean upper bound of the true r.

References

Altshuller, A. P., Ambient air hydroxyl radical concentrations: Measurements and model predictions, *JAPCA*, *39*, 704–708, 1989.

Callies, J., Absorptionsspektroskopischer Nachweis von Hydroxyl-Radikalen in der Troposphäre, Ph.D. thesis, Univ. of Cologne, Germany, 1988.

Comes, F. J., W. Armerding, R. Grigonis, A. Herbert, M. Spiekermann, and J. Walter, Tropospheric OH: Local measurements and their interpretations, *Ber. Bunsenges. Phys. Chem.*, *96*, 284–286, 1992.

Dodge, M. C., A comparison of three photochemical oxidant mechanisms, *J. Geophys. Res.*, *94*, 5121–5136, 1989.

Dorn, H.-P., J. Callies, U. Platt, and D. H. Ehhalt, Measurement of tropospheric OH concentrations by laser-long path absorption spectroscopy, *Tellus*, *40*(B), 437–445, 1988.

Ehhalt, D. H., Chemische Umwandlungen in der Atmosphäre, in *Forum der Rheinisch-Westfälischen Akademie der Wissenschaften*, p. 21, Westdeutscher Verlag, 1986.

Ehhalt, D. H., Free radicals in the atmosphere, *Free Radicals Res. Commun.*, *3*, 153–164, 1987.

Ehhalt, D. H., H.-P. Dorn, and D. Poppe, The chemistry of the hydroxyl radical in the troposphere, *Proc. R. Soc. Edinburgh*, *97*(B), 17–34, 1991.

Eisele, F. L., and D. J. Tanner, Ion-assisted tropospheric OH measurements, *J. Geophys. Res.*, *96*, 9295–9308, 1991.

Felton, C. C., A radiocarbon tracer method for measuring tropospheric OH, Ph.D. thesis, Washington State Univ., Seattle, 1988.

Felton, C. C., J. C. Sheppard, and M. J. Campbell, Measurements of the diurnal OH cycle by a ^{14}C-tracer method, *Nature*, *335*, 53–55, 1988.

Felton, C. C., J. C. Sheppard, and M. J. Campbell, The radiochemical hydroxyl radical measurement method, *Environ. Sci. Technol.*, *24*, 1841–1847, 1990.

Hewitt, C. N., and R. M. Harrison, Tropospheric concentrations of the hydroxyl radical—A review, *Atmos. Environ.*, *19*, 545–554, 1985.

Hofzumahaus, A., H.-P. Dorn, J. Callies, U. Platt, and D. H. Ehhalt, Tropospheric OH concentration measurements by laser long-path absorption spectroscopy, *Atmos. Environ.*, *25*(A), 2017–2022, 1991.

Hough, A., An intercomparison of mechanisms for the production of photochemical oxidants, *J. Geophys. Res.*, *93*, 3789–3812, 1988.

Junkermann, W., U. Platt, and A. Volz-Thomas, A photoelectric detector for the measurement of photolysis frequencies of ozone and other atmospheric molecules, *J. Atmos. Chem.*, *8*, 203–227, 1989.

Levy, II, H., Normal atmosphere: Large radical and formaldehyde predicted, *Science*, *173*, 141–143, 1971.

Levy, II, H., Photochemistry of the lower troposphere, *Planet. Space Sci.*, *20*, 919–935, 1972.

Liu, S. C., M. Trainer, F. C. Fehsenfeld, D. D. Parrish, E. J. Williams, D. W. Fahey, G. Hübler, and P. C. Murphy, Ozone production in the rural troposphere and the implications for the regionals and global ozone distribution, *J. Geophys. Res.*, *92*, 4191–4207, 1987.

Logan, J. A., M. J. Prather, S. C. Wofsy, and M. B. McElroy, Tropospheric Chemistry: A global perspective, *J. Geophys. Res.*, *86*, 7210–7254, 1981.

Martin, R. S., H. Westberg, E. Allwine, L. Ashman, J. C. Farmer, and B. Lamb, Measurement of isoprene and its atmospheric oxidation products in a central Pennsylvania deciduous forest, *J. Atmos. Chem.*, *13*, 1–32, 1991.

Middleton, P., W. R. Stockwell, and W. P. Carter, Aggregation and analysis of volatile organic compounds emissions for regional modelling, *Atmos. Environ.*, *24*(A), 1107–1133, 1990.

Mount, G. H., The measurement of tropospheric OH by long path absorption, 1, Instrumentation, *J. Geophys. Res.*, *97*, 2427–2444, 1992.

Mozurkewich, M., P. H. McMurry, A. Gupta, and J. G. Calvert, Mass accommodation coefficient for HO_2 radicals on aqueous particles, *J. Geophys. Res.*, *92*, 4163–4170, 1987.

Perner, D., U. Platt, M. Trainer, G. Hübler, J. Drummond, W. Junkermann, J. Rudolph, B. Schubert, A. Volz, D. H. Ehhalt, J. Rumpel, and G. Helas, Measurements of tropospheric OH concentrations: A comparison of field data with model predictions, *J. Atmos. Chem.*, *5*, 185–216, 1987.

Platt, U., M. Rateike, W. Junkermann, A. Hofzumahaus, and D. H. Ehhalt, Detection of atmospheric OH radicals, *Free. Radicals Res. Commun.*, *3*, 165–172, 1987.

Platt, U., M. Rateike, W. Junkermann, J. Rudolph, and D. H. Ehhalt, New tropospheric OH measurements, *J. Geophys. Res.*, *93*, 5159–5166, 1988.

Poppe, D., M. Wallasch, J. Zimmermann, H.-P. Dorn, and D. H. Ehhalt, Comparison of the tropospheric concentration of OH with model calculations, *Ber. Bunsenges. Phys. Chem.*, *96*, 286–290, 1992.

Poppe, D., M. Wallasch, and J. Zimmermann, The dependence of the concentration of OH on its precursors under moderately polluted conditions: A model study, *J. Atmos. Chem.*, *16*, 61–78, 1993a.

Poppe, D., et al., Measurements of atmospheric trace gas concentrations during the OH-campaign in Jülich 1988, *KFA Jülich Rep. 2731*, Forschungszentrum, Jülich, Germany, 1993b.

Poppe, D., J. Zimmermann, and D. H. Ehhalt, OH concentrations in the planetary boundary layer: A comparison between field data and model calculations, *KFA Jülich Rep.*, Jülich, Germany, in press, 1994.

Röth, E. P., Description of a photon-flux model, *KFA Jülich Rep.*, Jülich, Germany, in press, 1994.

Schneeweiß, H., and H. J. Mittag, *Lineare Modelle mit fehlerbehafteten Daten*, Physica Verlag, Heidelberg, Germany, 1986.

Sillman, S., J. A. Logan, and S. C. Wofsy, The sensitivity of ozone

to nitrogen oxides and hydrocarbons in regional ozone episodes, *J. Geophys. Res.*, *95*, 1837–1851, 1990.

Stockwell, W. R., P. Middleton, J. S. Chang, and X. Tang, The second generation regional acid deposition model chemical mechanism for regional air quality modeling, *J. Geophys. Res.*, *95*, 16,343–16,367, 1990.

Thompson, A. M., M. A. Huntley, and R. W. Stewart, Perturbations to tropospheric oxidants, 1985–2035, 1, Calculations of ozone and OH in chemically coherent regions, *J. Geophys. Res.*, *95*, 9829–9844, 1990.

Wallasch, M., D. Poppe, D. Brüning, H.-P. Dorn, R. Koppmann, K.-P. Müller, F. Rohrer, J. Rudolph, U. Schmidt, and D. H. Ehhalt, Trace gas abundances during a summer period 1988 in Jülich (Germany), *KFA Jülich Rep.*, Jülich, Germany, in press, 1994.

Weinstock, B., H. Niki, and T. Y. Chang, Chemical factors affecting the hydroxyl radical concentration in the troposphere, *Adv. Environ. Sci. Technol.*, *10*, 221–258, 1980.

Withby, K. T., The physical characteristics of sulfur aerosols, *Atmos. Environ.*, *12*, 135–159, 1978.

R. Bauer, T. Brauers, D. Brüning, J. Callies, H.-P. Dorn, D. H. Ehhalt, A. Hofzumahaus, F.-J. Johnen, A. Khedim, H. Koch, R. Koppmann, H. London, K.-P. Müller, R. Neuroth, C. Plass-Dülmer, U. Platt, D. Poppe, F. Rohrer, E.-P. Röth, J. Rudolph, U. Schmidt, M. Wallasch, and J. Zimmermann, Institute for Atmospheric Chemistry, Forschungszentrum Jülich, P. O. Box 1913, D-52425 Jülich, Germany.

(Received August 6, 1993; revised January 20, 1994;
accepted February 3, 1994.)